

Sources and sinks of dissolved inorganic carbon in an urban tropical coastal bay revealed by $\delta^{13}\text{C}$ -DIC signals

Luiz C. Cotovicz Jr.^{a,b,*}, Bastiaan A. Knoppers^a, Loris Deirmendjian^b, Gwenaël Abril^{a,b,c}

^a Programa de Geoquímica, Universidade Federal Fluminense, Niterói, RJ, Brazil

^b Laboratoire, Environnements et Paléoenvironnements Océaniques et Continentaux (EPOC) UMR 5805, CNRS – Université de Bordeaux, Pessac, France

^c Biologie des Organismes et Ecosystèmes Aquatiques (BOREA), UMR 7208, Muséum National d'Histoire Naturelle, CNRS, SU, UCN, UA, IRD, 61 rue Buffon, 75231, Paris cedex 05, France

ARTICLE INFO

Keywords:

$\delta^{13}\text{C}$ -DIC signatures
Coastal eutrophication
Carbon cycling
Guanabara bay

ABSTRACT

Dissolved inorganic carbon (DIC), its stable isotope composition ($\delta^{13}\text{C}$ -DIC) and ancillary parameters of the water column were investigated in a eutrophic tropical marine-dominated estuary surrounded by a large urban area (Guanabara Bay, Rio de Janeiro, Brazil). Most negative $\delta^{13}\text{C}$ -DIC signatures (down to -6.1‰) were found in polluted regions affected by direct sewage discharges where net heterotrophy induces high partial pressure of CO_2 ($p\text{CO}_2$) and DIC concentrations. Keeling plot was applied to this polluted region and determined the $\delta^{13}\text{C}$ -DIC sewage signature source of -12.2‰ , which is very consistent with isotopic signature found in wastewater treatment plants. These negative $\delta^{13}\text{C}$ -DIC signatures (i.e., DIC depleted in ^{13}C) were restricted to the vicinity of urban outlets, whereas in the largest area of the bay $\delta^{13}\text{C}$ -DIC signatures were more positive (i.e., DIC enriched in ^{13}C). The most positive $\delta^{13}\text{C}$ -DIC signatures (up to 4.6‰) were found in surface waters dominated by large phytoplankton blooms, with positive correlation with chlorophyll *a* (Chl *a*). In the largest area of the bay, the preferential uptake of the lighter stable carbon isotope (^{12}C) during photosynthesis followed the Rayleigh distillation, and appeared as the most important driver of $\delta^{13}\text{C}$ -DIC variations. This reveals an important isotopic fractionation (ϵ) by phytoplankton due to successive algal blooms that has turned the remaining DIC pool enriched with the heavier stable carbon isotope (^{13}C). The calculated diel apparent ϵ showed higher values in the morning (18.7‰ – 21.6‰) and decreasing in the afternoon (6.8‰ – 11.1‰). ϵ was positively correlated to the $p\text{CO}_2$ ($R^2 = 0.88$, $p = 0.005$) and DIC concentrations ($R^2 = 0.73$, $p = 0.02$), suggesting a decline in carbon assimilation efficiency and decreasing uptake of the lighter carbon under CO_2 limiting conditions. The eutrophic coastal waters of Guanabara Bay have $\delta^{13}\text{C}$ -DIC signatures well above that found in estuaries, shelf and ocean waters worldwide.

1. Introduction

The coastal zone is one of the most biologically active areas of the biosphere, and plays an important role in the global carbon cycle (Gattuso et al., 1998). Estuaries are considered prominent coastal environments, which receive large amounts of organic matter from land, and exchange material with the adjacent ocean and the atmosphere (Borges and Abril, 2011; Chen et al., 2013). The most recent global estimation of estuarine CO_2 emissions to the atmosphere is about 0.1 Pg C yr^{-1} (Chen et al., 2013). These emissions occur because in estuaries the consumption of organic carbon exceeds net primary production, and the net heterotrophy in the ecosystem leads to high $p\text{CO}_2$ levels (Gazeau et al., 2004; Borges and Abril, 2011), together with lateral CO_2 inputs from tidal wetlands (Cai and Wang 1998., Bouillon

et al., 2003; Bouillon et al. 2011) and rivers (Frankignoulle et al. 1998; Hunt et al. 2010; Joesoef et al. 2017). However, it must be highlighted that the high diversity of estuarine morphological types and associated ecosystems creates strong local and regional differences that hinders the extrapolation of results for global estimations, which remain uncertain (Borges, 2005).

The $\delta^{13}\text{C}$ -DIC is a helpful tool for understanding biogeochemical cycling and tracing the sources, sinks and transformations of carbon in aquatic ecosystems (Gillikin et al., 2006; Burt et al., 2016). During photosynthesis, plants use preferentially the lighter stable carbon isotope (^{12}C) than the heavier stable carbon isotope (^{13}C). This stable carbon isotope discrimination leads to an isotopic fractionation and, thus, organic carbon in marine plants and algae are depleted in ^{13}C relative to their DIC source (Burkhardt et al., 1999). Therefore, aquatic

* Corresponding author. Instituto de Ciências do Mar, Universidade Federal do Ceará, Fortaleza, CE, Brazil.
E-mail address: lccjunior@id.uff.br (L.C. Cotovicz).

<https://doi.org/10.1016/j.ecss.2019.02.048>

Received 27 November 2018; Received in revised form 27 February 2019; Accepted 28 February 2019

Available online 05 March 2019

0272-7714/ © 2019 Elsevier Ltd. All rights reserved.

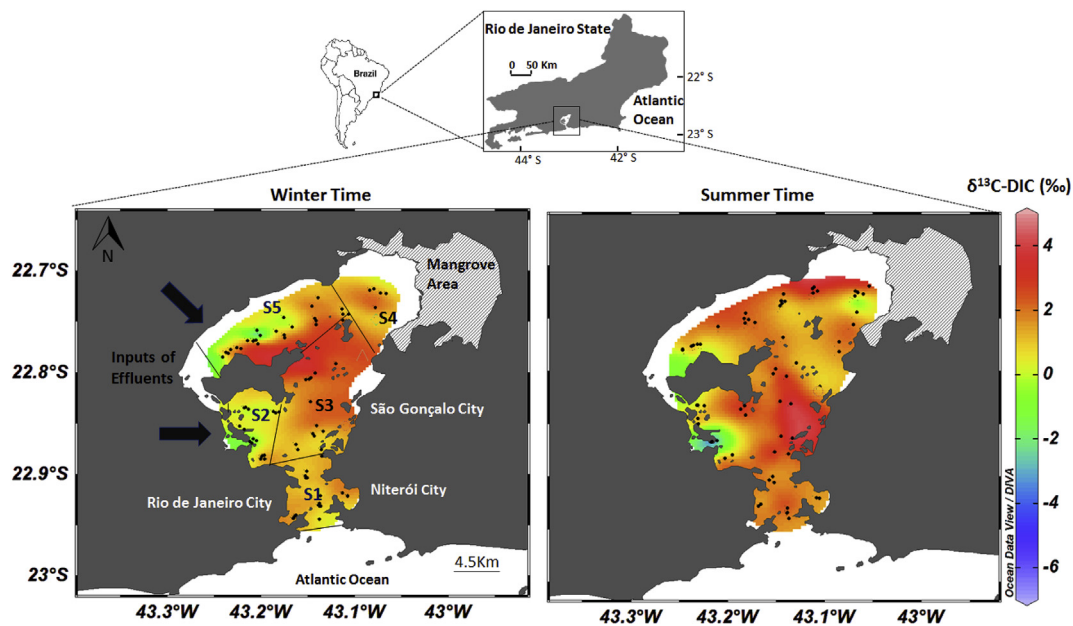


Fig. 1. Composite maps showing the study area and the spatial distributions of the $\delta^{13}\text{C-DIC}$ signatures in winter period (a) and summer period (b) in surface waters of the Guanabara Bay. The bay was divided into five sectors (S1 to S5). The black dots represent the sampled sites.

primary production tends to leave the water rich in ^{13}C , increasing $\delta^{13}\text{C-DIC}$ signatures (Zeebe and Wolf-Gladrow, 2001). On the other hand, the degradation of organic carbon by respiring heterotrophic organisms, either in pelagic or in benthic compartments, produces CO_2 with approximately the same isotopic signature of the respired organic matter, decreasing $\delta^{13}\text{C-DIC}$ signatures (Kendall and Doctor, 2004; Miyajima et al., 2009; Bouillon et al. 2011; Bhavya et al., 2018).

The freshwater $\delta^{13}\text{C-DIC}$ endmember in estuaries could present very different values, and related to distinct isotopic signatures from the major sources and sinks, including biogenic and lithological sources, air-water CO_2 exchanges, and *in situ* metabolism (Mook and Tan, 1991; Campeau et al., 2017). This large heterogeneity leads to freshwater endmembers generally ranging between -5‰ and -25‰ , depending on the intensity of the different $\delta^{13}\text{C-DIC}$ sources and sinks (Kendall and Doctor, 2004; Finlay and Kendall, 2007). This results in marked changes in the stable isotope carbon composition across estuarine salinity gradients from freshwater to the sea (Fry, 2002). Very negative $\delta^{13}\text{C-DIC}$ signatures (down to -20‰), which shows a strong depletion of ^{13}C in the DIC pool, were documented in several estuaries, especially at low salinity regions, which are usually highly heterotrophic (Bouillon et al., 2007; Bouillon et al. 2011). Contrary to low salinity regions, the marine-dominated regions of estuaries exhibit higher $\delta^{13}\text{C-DIC}$ signatures that are usually in the range of -2‰ to $+2\text{‰}$ (mean approaching 0‰) due to a predominance of marine DIC and a limited influence of DIC from terrestrial sources (Mook and Tan, 1991; Chanton and Lewis, 1999; Gruber et al., 1999). Generally, the stable isotope signature of DIC in estuaries follows mixing process between marine and freshwater end-members (Mook and Tan, 1991), attesting that DIC levels are mainly controlled by physical processes (Wang et al., 2016). However, deviation from mixing curves are frequently reported (Coffin and Cifuentes, 1999; Bouillon et al., 2003; Gillikin et al., 2006; Miyajima et al., 2009; Bouillon et al. 2011; Bhavya et al., 2018). The $\delta^{13}\text{C-DIC}$ data below conservative mixing suggest prevalence of respiration that adds depleted $\delta^{13}\text{C-DIC}$ (Bouillon et al., 2003; Bouillon et al. 2011). On the other hand, in estuaries with important levels of photosynthesis, deviation above to the mixing curve can occur due to the preferential uptake of the lighter stable carbon isotope (Coffin and Cifuentes, 1999; Zeebe and Wolf-Gladrow, 2001; Gillikin et al., 2006). In addition to the metabolic controls (respiration and photosynthesis), the $\delta^{13}\text{C-DIC}$ dynamic is also affected by physical controls such as the

CO_2 exchange with the atmosphere and dissolution/precipitation of carbonate minerals (Finlay and Kendall, 2007). It is important to point out that when DIC reaches the equilibrium with atmospheric CO_2 concentrations, the $\delta^{13}\text{C-DIC}$ becomes close to the value of 0‰ (Bouillon et al. 2011). However, there is an important temperature-dependent equilibrium isotope fractionation of $\delta^{13}\text{C-DIC}$ (Zhang et al., 1995), and this can cause regional deviations from 0‰ depending on aquatic and atmospheric temperatures.

In addition to the high natural variability of $\delta^{13}\text{C-DIC}$ values in estuaries and coastal zones, the isotopic signature of the DIC can change in response to anthropogenic forcing (Finlay and Kendall, 2007; Yang et al., 2018). Human activities, such as land-use changes, wastewater discharges, and wetlands destruction, are altering carbon sources, sinks, cycling and budgets (Bauer et al., 2013). Although the use of $\delta^{13}\text{C-DIC}$ is well established for investigations of ecosystem metabolism and water mixing processes in estuaries, this parameter has been rarely used to describe the occurrence of anthropogenic perturbations such as eutrophication. In the tropics, the development of coastal megacities with inefficient treatment of wastewaters, combined with enhanced biological activity due to specific climatic features, leads to drastic modifications of the regional carbon cycle (Carreira et al., 2002; Cotovicz et al., 2015), which should impact the isotopic signature of the DIC. Here, we present the first measurements of $\delta^{13}\text{C-DIC}$ in a tropical coastal embayment that receives large amounts of untreated wastewaters from surrounding urban areas, which hosts a population of about 9 millions of inhabitants. Large inputs of domestic effluents into the bay enhanced the levels of aquatic primary production (Rebello et al., 1988), and turned the bay into a marked sink of CO_2 (Cotovicz et al., 2015). We hypothesized that these human perturbations of the estuarine system will have important impacts on the isotopic signature of the DIC that need a detailed characterization. We also expected uncommon isotopic signatures of these coastal waters compared to other estuarine and marine environments.

2. Materials and methods

2.1. Study area

Guanabara Bay ($22^\circ41'–22^\circ58' \text{S}$ and $43^\circ02'–43^\circ18' \text{W}$) is a tropical coastal embayment located at the SE-Brazilian coast (Fig. 1). The

surface area is 384 km², the mean depth is 5.7 m, and the water volume is about 1870 × 10⁶ m³. The bay has a microtidal regime, and is a partially mixed estuary (Kjerfve et al., 1997), but under conditions of high solar incidence and high freshwater discharge the bay could present a strong vertical thermohaline stratification (Cotovicz et al., 2015). The annual freshwater inputs by the rivers is only about 100 m³ s⁻¹ (Kjerfve et al., 1997). The large difference between the high water volume and the low amount of freshwater inputs are reflected in high salinities along the Bay (averaging 29.5 ± 4.8), with few lower values (down to 15) at the vicinity of the small river mouths. Considering the bay as a whole, more than 85% of the water volume corresponds to seawater, whereas only 15% is attributed to freshwaters (Costa-Santos, 2015). The average time necessary to renew 50% of the total water volume with the tidal movements is 11.4 days, but with significant spatial differences, especially at the most confined regions (Kjerfve et al., 1997). Guanabara Bay is located in the intertropical zone, and the climate is characterized by a warm and wet summer, and a cooler and drier winter (Bidone and Lacerda, 2004). The annual freshwater input to the bay is approximately 100 ± 59 m³ s⁻¹, and modest compared to the bay's water volume, which contributed to the predominance of polyhaline to euhaline waters. The bay is one of the most polluted coastal systems in the world that receives large inputs of untreated domestic and industrial effluents at approximately 25 m³ s⁻¹ (Kjerfve et al., 1997; Bidone and Lacerda, 2004). We compartmentalized the bay into five domains (sectors 1, 2, 3, 4, and 5) as described by Cotovicz et al. (2015; 2018a) for the treatment, computations and interpretation of the data (Fig. 1).

2.2. Experimental design, sampling procedures and laboratory analysis

Between 2013 and 2014, nine sampling campaigns were conducted for the analysis of δ¹³C-DIC and ancillary parameters of the water column in Guanabara Bay. The water parameters were sampled in continuous on-line and/or discrete procedures. Continuous measurements were performed to analyze the water temperature, salinity, DO and pCO₂, as described by Cotovicz et al. (2015). Briefly, one submersible water pump was positioned at the side of the boat (depth of 0.5 m), providing continuous water flow to a measurement system located inside the boat. The continuous measurements of pCO₂ followed the equilibration technique using a marble-type equilibrator coupled to a non-dispersive infrared gas detector (LICOR 820) (Frankignoulle et al., 2001; Cotovicz et al., 2016a). The equilibrator had a response time lower than 4 min, and, as the boat speed during measurements was about 6 km h⁻¹, pCO₂ measurements were averaged over approximately 300 m of the boat's track. One calibrated YSI 6600 V2 multi-parameter probe measured continuously the water temperature, salinity and DO.

Discrete water samples were taken for δ¹³C-DIC, chlorophyll *a* (Chl *a*), phaeopigments, total alkalinity (TA), and dissolved inorganic phosphorus (PO₄³⁻), accounting to about 16–19 stations distributed across the bay, except in December 2013, when only 8 stations could be sampled. Sub-surface water samples were collected at 0.5 m depth with a Niskin bottle, and conditioned (i.e. fixed and/or kept on ice in the dark) for further chemical analysis at the laboratory. The comparison between surface and bottom waters in terms of δ¹³C-DIC concentrations and other physico-chemical parameters were performed at some stations, during the summer period, and during conditions of maximal vertical stratification at summer period in sectors 3, 4, and 5 (Cotovicz et al., 2016b).

The water was filtered with whatman GF/F glass-fibre filters (porosity 0.45 μm) followed by determination of suspended particulate material (SPM), Chl *a* and phaeopigments. The filters were pre-combusted (at 500 °C during 6 h) and pre-weighted before utilization. After filtration, filters were dried in an oven at 50 °C and then weighed. SPM was determined gravimetrically. Chl *a* and phaeopigments were extracted in 90% acetone and quantified spectrophotometrically before

and after acidification of the samples, according to Strickland and Parsons (1972). PO₄³⁻ was quantified by the colorimetric method as in Grasshoff et al. (1999). For the stable isotope composition of the DIC, the water was sampled and transferred directly to 150 mL serum vials, which were poisoned by adding 0.2 mL of a solution saturated with HgCl₂ and carefully sealed, taking care that no air remained in contact with samples. Vials were also stored in the dark to prevent photo oxidation. In the laboratory, the δ¹³C-DIC signature was determined following the protocol of Bouillon et al. (2007). We injected 40 mL of helium gas inside the bottles to create a headspace, maintaining the bottles bottom-up and simultaneously expelling water by a second needle. Then, 0.2 mL of ultrapure and concentrated H₃PO₄ was introduced to convert all inorganic carbon to CO₂. Samples were shaken vigorously and kept 12 h in the dark at a controlled temperature of 25 °C. The δ¹³C of CO₂ in the headspace was determined by injecting between 0.5 mL and 1 mL of the headspace gas in an isotopic ratio mass spectrometer (IRMS, Micromass IsoPrime), equipped with a manual gas injection port. δ¹³C-DIC was calibrated using a laboratory standard, which was prepared adding 45 mg of Na₂CO₃ in a sealed vial flushed with helium and dissolved with 3 mL of 85% H₃PO₄, as described in Deirmendjian and Abril (2018). This standard was calibrated against certified standard (NBS19, -1.96 ‰) using a dual-inlet IRMS. The isotopic value of the Na₂CO₃ standard was -4.5 ± 0.2‰. The obtained δ¹³C values were corrected for the partitioning of CO₂ between the gaseous (headspace) and water phase in each sample using the algorithm of Miyajima et al. (1995). The reproducibility of the analysis was approximately 0.1‰. The δ¹³C-DIC signatures are reported in ‰ relative to the standard Vienna Pee Dee Belemnite (V-PDB) scale. TA was measured on 70 mL of filtrate samples, by the classical Gran titration method (Gran, 1952) using an automated titration system (Mettler Toledo model T50). The reproducibility of the titration was ± 3 μmol kg⁻¹ (n = 5), and the accuracy was estimated at ± 5 μmol kg⁻¹ (inferred from certified material reference, CRM, provided by A. G. Dickson, Scripps institution of Oceanography). To compare the pCO₂ with discrete sampling, we used the value of pCO₂ exactly the moment of the discrete sampling at the fixed station (after achievement of equilibration). As such, we obtained the values of pCO₂ and TA at same time and place. DIC concentrations were calculated from the values of pCO₂ and TA, and were very consistent with the DIC calculated from the values of measured pH and TA (Cotovicz et al., 2015). Calculations of DIC were made using the carbonic acid constants proposed by Mehrbach et al. (1973) refitted by Dickson and Millero (1987) as implemented in the CO2Calc V 4.0.9 program (Robbins et al., 2010).

2.3. Calculation of DIC and δ¹³C-DIC addition or loss

Guanabara Bay did not present a marked saline gradient (Table 1; range was 14–35). Instead, this bay presents salinities generally higher than 30, and the low salinity waters are restricted to locations close to the river water and effluent discharges. When the river DIC inputs are weak or negligible, the conservative mixing of DIC (DIC_{mixing}) can be calculate using the marine end-member as follows (Jiang et al., 2008):

$$\text{DIC}_{\text{mixing}} = S_i/S_{\text{ocean}} \times \text{DIC}_{\text{ocean}} \quad (1)$$

Where S_i is the measured salinity, S_{ocean} the salinity of the ocean end-member, and $\text{DIC}_{\text{ocean}}$ the DIC concentration of the ocean end-member. The $\text{DIC}_{\text{mixing}}$ is the DIC concentration after the ocean end-member is diluted by a zero DIC freshwater; however, this equation also includes possible DIC inputs from river (Jiang et al., 2008).

The excess of DIC ($\Delta\text{DIC}_{\text{excess}}$) is defined as the DIC addition or loss relative to the conservative mixing (Jiang et al., 2008), and can be expressed as:

$$\Delta\text{DIC}_{\text{excess}} = \text{DIC}_i - \text{DIC}_{\text{mixing}} \quad (2)$$

Where DIC_i is the measured DIC. In the same way, the excess of total

Table 1Mean (\pm standard deviation) and ranges of the principal parameters investigated in the waters of Guanabara Bay, separated by sectors.s

	Sector 1	Sector 2	Sector 3	Sector 4	Sector 5
Temperature ($^{\circ}$ C)	23.8 \pm 1.7 (21.0–29.3)	25.5 \pm 2.2 (22.1–32.4)	25.4 \pm 2.1 (22.1–31.5)	26.8 \pm 2.6 (22.0–32.3)	26.7 \pm 2.2 (22.6–33.9)
Salinity	32.2 \pm 2.1 (25.4–34.9)	30.3 \pm 2.4 (17.7–33.7)	29.8 \pm 3.0 (15.1–33.8)	27.0 \pm 4.3 (14.6–33.2)	27.2 \pm 3.5 (16.6–32.9)
$\delta^{13}\text{C-DIC}$ (‰)	1.59 \pm 0.84 (–0.02/3.03)	0.43 \pm 1.93 (–6.17/3.24)	1.68 \pm 1.25 (–1.88/4.57)	1.15 \pm 1.50 (–2.50/3.81)	(0.99 \pm 1.66) (–4.87/3.71)
$p\text{CO}_2$ (ppmv)	411 \pm 145 (104–747)	711 \pm 561 (50–3715)	286 \pm 157 (41–660)	307 \pm 256 (29–2222)	272 \pm 293 (22–2203)
pH (NBS)	8.20 \pm 0.16 (7.90–8.71)	8.15 \pm 0.32 (7.33–8.96)	8.35 \pm 0.23 (7.88–8.96)	8.34 \pm 0.29 (7.39–9.01)	8.44 \pm 0.31 (7.51–9.23)
TA ($\mu\text{mol.kg}^{-1}$)	2240 \pm 92 (1942–2320)	2291 \pm 99 (1890–2488)	2168 \pm 177 (1507–2500)	2045 \pm 369 (2111–3920)	2137 \pm 166 (1479–2314)
DIC ($\mu\text{mol.kg}^{-1}$)	1985 \pm 120 (1720–2127)	2044 \pm 268 (1526–2523)	1847 \pm 257 (1332–2290)	1658 \pm 259 (1095–2118)	1758 \pm 264 (1198–2190)
DO (%)	103 \pm 29 (48–221)	97 \pm 59 (2–263)	138 \pm 51 (56–357)	142 \pm 62 (30–361)	160 \pm 69 (46–370)
Chl- α ($\mu\text{g.L}^{-1}$)	19.1 \pm 22.0 (2.0–128.0)	46.2 \pm 51.4 (3.3–212.9)	57.6 \pm 90.0 (1.6–537.2)	69.2 \pm 60.2 (13.1–288.8)	107.7 \pm 101.8 (1.5–822.1)
$\text{PO}_4^{3-}\text{-P}$ (μM)	1.11 \pm 0.60 (0.11–2.44)	5.28 \pm 3.88 (0.17–20.79)	1.51 \pm 1.07 (0.17–1.10)	1.10 \pm 0.79 (0.03–2.96)	2.23 \pm 2.17 (0.02–8.72)

alkalinity ($\Delta\text{TA}_{\text{excess}}$) can be calculated as the deviation from the conservative mixing:

$$\Delta\text{TA}_{\text{excess}} = \text{TA}_i - \text{TA}_{\text{mixing}} \quad (3)$$

In a similar approach developed by Yang et al. (2018), the difference between the $\delta^{13}\text{C-DIC}$ of the sample ($\delta^{13}\text{C-DIC}_i$) and the $\delta^{13}\text{C-DIC}$ of the marine end-member ($\delta^{13}\text{C-DIC}_{\text{ocean}}$) represent the stable isotopic deviation from the marine end-member ($\Delta\delta^{13}\text{C-DIC}$) linked to local processes, as follows:

$$\Delta\delta^{13}\text{C-DIC} = \delta^{13}\text{C-DIC}_i - \delta^{13}\text{C-DIC}_{\text{ocean}} \quad (4)$$

When DIC is altered by processes of organic carbon degradation, primary production, and/or air-water exchanges, its isotopic composition is also altered, following mass balance equations (complete set of equation can be found in Yang et al., 2018). The simplified equation is:

$$\Delta\delta^{13}\text{C-DIC} = \Delta\text{DIC}_{\text{excess}}/\text{DIC}_i * (\delta^{13}\text{C}_{\text{excess}} - \delta^{13}\text{C}_{\text{ocean}}) \quad (5)$$

The $\delta^{13}\text{C}_{\text{excess}}$ represent the stable isotopic composition of the added or lost DIC whereas the $\delta^{13}\text{C}_{\text{ocean}}$ is the stable isotopic composition of the marine end-member. In coastal waters with limited river inputs, the DIC_i and $\text{DIC}_{\text{ocean}}$ are approximately the same. Then, equation (5) can be adjusted to:

$$\Delta\delta^{13}\text{C-DIC} = \Delta\text{DIC}_{\text{excess}}/\text{DIC}_{\text{ocean}} * (\delta^{13}\text{C}_{\text{excess}} - \delta^{13}\text{C}_{\text{ocean}}) \quad (6)$$

This equation above means that $\Delta\text{DIC}_{\text{excess}}/\text{DIC}_{\text{ocean}}$ and $\Delta\delta^{13}\text{C-DIC}$ are linked and linearly related. In this way, the slope of this relationship can be used to infer the isotopic composition of the added or lost DIC and the ocean end-member value (Yang et al., 2018).

The $\delta^{13}\text{C}$ signature of the added or lost DIC due to the organic carbon production or respiration was taken as the average of $\delta^{13}\text{C-POC}$ value in the bay, which is about -20‰ (Kalas et al., 2009). The fractionation factor (α_{CO_2}) due to outgassing of CO_2 was calculated following the procedures described by Alling et al. (2012) and Samanta et al. (2015). We applied the equation of Rau et al. (1996) to estimate the fractionation factor (α) between DIC and the dissolved CO_2 in water, according to:

$$\delta^{13}\text{C-CO}_2 = \delta^{13}\text{C-DIC} + 23.644 - 9701.5/T \quad (7)$$

This equation gives the equilibrium fractionation factor (ϵ_{CO_2}), which is the difference between $\delta^{13}\text{C-CO}_2$ and $\delta^{13}\text{C-DIC}$. This calculation provides a value of ϵ_{CO_2} of -9.2‰ , representing the averaged found in the sector 2 (the only sector that is a net source of CO_2 to the atmosphere). Defining $f\text{CO}_2$ as the fraction of DIC remaining in the water after outgassing of CO_2 , we can calculate the DIC concentration after CO_2 loss (DIC_F , which is equivalent to the measured DIC, DIC_i), according:

$$\text{DIC}_F = f\text{CO}_2 * \text{DIC}_i \quad (8)$$

Where DIC_i represents the initial DIC concentration before outgassing, which is equivalent to the calculated DIC based on equation (1), $\text{DIC}_{\text{mixing}}$. The $^{13}\text{C}/^{12}\text{C}$ ratio in the remaining waters (R_F) will be

fractionated during progressive outgassing by the Rayleigh distillation process, according:

$$R_F = R_i (f\text{CO}_2)^{\alpha_{\text{CO}_2} - 1} \quad (9)$$

Where R_i is the initial $^{13}\text{C}/^{12}\text{C}$ ratio before outgassing. This equation is equivalent to (Alling et al., 2012):

$$\delta^{13}\text{C}_F = \delta^{13}\text{C}_i + 10^3 (\alpha_{\text{CO}_2} - 1) \ln(f\text{CO}_2) \quad (10)$$

If we consider that the amount of DIC that is lost by outgassing is small compared to the total pool of DIC (Alling et al., 2012; Samanta et al., 2015), the DIC_F tend to be close to $\text{DIC}_{\text{mixing}}$ (in fact this ratio is close to 1 in Guanabara Bay, and consistent with other studies). In this way, equations (1), (4), (8) and (9) can be combined:

$$\Delta\delta^{13}\text{C-DIC} \sim \Delta\text{DIC}_{\text{excess}} (\alpha_{\text{CO}_2} - 1) 10^3 \quad (11)$$

Considering that $\alpha_{\text{CO}_2} \sim 0.991$ in Guanabara Bay, there is a near linear relationship between $\Delta\delta^{13}\text{C-DIC}$ and $\Delta\text{DIC}_{\text{excess}}$, with a slope of -9.2 value of outgassed CO_2 . As the bay is a net sink of CO_2 (Cotovicz et al., 2015), we also calculate a slope representing the uptake of atmospheric CO_2 . During uptake, $\alpha_{\text{CO}_2} \sim 0.998$ (Siegenthaler and Münnich, 1981; Inoue and Sugimura, 1985), giving a slope of approximately -2.0 that represents the process of CO_2 uptake.

The average $\delta^{13}\text{C}$ -DIC signature of the wastewater DIC input was calculate with the keeling plot for the most polluted region (Fig. S1, supplementary file), which give a value of -12.2‰ . This stable isotopic signature is very consistent with that found in wastewater samples (-12.0‰).

2.4. Estimates of the apparent photosynthetic fractionation factor of DIC ($\epsilon\text{-DIC}$)

Photosynthesis leads to the ^{13}C enrichment of the remaining DIC pool as the phytoplankton uses preferentially the ^{12}C (Mook, 2001). The apparent photosynthetic fractionation factor of DIC consumed ($\epsilon_p\text{-DIC}$) was calculated using the diurnal variations in the DIC concentrations and its stable isotope composition. In Sep. 2013, Jan.2014 and Apr. 2014, diurnal variations in water $\delta^{13}\text{C-DIC}$ were estimated within the upper sectors (sector 4 and 5) by performing lateral trajectories back and forth across the sectors from dawn to noon (further referred as morning period) and from noon to dusk (further referred as afternoon period). The stable isotope composition of the DIC used by phytoplankton ($\delta^{13}\text{C}_{\text{used}}$) from dawn to noon period is likened to the DIC concentrations and its stable isotope composition observed between these two periods considering a simple conservative mixing by a mass balance equation:

$$\delta^{13}\text{C}_{\text{used}} = (\text{DIC}_{\text{dawn}}\delta^{13}\text{C}_{\text{dawn}} - \text{DIC}_{\text{noon}}\delta^{13}\text{C}_{\text{noon}}) / (\text{DIC}_{\text{dawn}} - \text{DIC}_{\text{noon}}) \quad (12)$$

Where $\delta^{13}\text{C}_{\text{dawn}}$ and $\delta^{13}\text{C}_{\text{noon}}$ refer to the stable isotope composition of the DIC at dawn and noon, respectively, and DIC_{dawn} and DIC_{noon} refer to their respective concentrations. This formulation was also applied to investigate the stable isotope composition of the DIC used by

phytoplankton during the afternoon. Then, this apparent photosynthetic fractionation of DIC (ϵ_p -DIC) was then estimated as the difference between the initial composition of DIC ($\delta^{13}\text{C}$ -DIC_i) and the calculated $\delta^{13}\text{C}_{\text{used}}$ for each period (morning and afternoon), as follows:

$$\epsilon_p\text{-DIC} = \delta^{13}\text{C}\text{-DIC}_i - \delta^{13}\text{C}_{\text{used}} \quad (13)$$

In addition, we calculated the plots of Rayleigh Distillation, where the increase in $\delta^{13}\text{C}$ -DIC was plotted against the consumed DIC at the diel scale, in a similar approach of Van Dam et al. (2018).

2.5. Statistical analysis

The Shapiro-Wilk test showed that data of $p\text{CO}_2$, TA, DIC, $\delta^{13}\text{C}$ -DIC and Chl *a* did not follow a normal distribution. Consequently, non-parametric statistical tests were performed. The paired Wilcoxon test was used to compare concentrations of the measured parameters between surface and bottom waters. The seasonal differences were analyzed by the Mann-Whitney test. Spearman rank coefficient was used to calculate the coefficient correlations between the measured parameters. Linear and non-linear (second order polynomial) regressions were also calculated. All statistical analysis were based on $\alpha = 0.05$ and were performed with the GraphPad Prism 6 software.

2.6. Data compilation and literature survey

A compilation of $\delta^{13}\text{C}$ -DIC signatures from global databases such as the *Institute National des Sciences de L'Univers* (INSU-France) and the Carbon Dioxide Information Analysis Center (CDIAC) was carried out to obtain $\delta^{13}\text{C}$ -DIC data of other estuarine, coastal and open ocean waters worldwide. We also used the search engines Google Scholar and Web of Science to compile data from literature. We recorded the available data directly from tables and/or interpolated from figures using the data extraction program PlotDigitalizer. The different $\delta^{13}\text{C}$ -DIC data obtained from this compilation work were ranked according to their salinity in order to compare it with the data obtained in this study.

3. Results

Table 1 shows the average concentrations with standard deviations as well as the ranges of the main water parameters analyzed in this study, separated by sectors. The upper sectors of the bay (sectors 4 and 5) presented lower salinities (27 ± 4.3 and 27.2 ± 3.5 , respectively) and higher temperatures (26.8 ± 2.6 °C and 26.7 ± 2.2 °C, respectively), associated to waters with longest residence times (Table 1). To the contrary of upper sectors, sector 1 which is located near the mouth of the bay, showed lower temperatures (23.8 ± 1.7 °C) and higher

salinities (32.2 ± 2.1) as expected due to the major influence of shelf waters.

The $\delta^{13}\text{C}$ -DIC signatures in Guanabara Bay did not present conservative distributions with salinity gradient (Fig. S2; supplementary file). Indeed, DIC in the bay was enriched in ^{13}C in some parts (mainly sectors 3, 4 and 5) relative to the marine end-member that presented a stable isotopic signature of 1.5‰ (Table 1), whereas in some restricted parts the bay showed ^{13}C depletion (mainly sector 2) (Table 1, Fig. 1). Spatially, the sectors 1 and 3 presented the higher averages of $\delta^{13}\text{C}$ -DIC signatures, which were 1.6‰ and 1.7‰, respectively (Table 1). However, some extreme high values ($\delta^{13}\text{C}\text{-DIC} > 3\text{‰}$) were also present at the most shallow-confined regions of the bay (sectors 4 and 5) (Table 1). Sector 2, the most polluted region, presented the lowest average of $\delta^{13}\text{C}$ -DIC, which was 0.4‰ (Table 1). Some more negative values of $\delta^{13}\text{C}$ -DIC were also found in sectors 4 and 5 close to the outlet of rivers and urban sewage networks (Table 1; Fig. 1). Considering all sectors, the range of $\delta^{13}\text{C}$ -DIC signature in the entire bay was -6.1‰ (Sector 2) to 4.6‰ (Sector 3). Temporally, the $\delta^{13}\text{C}$ -DIC also showed important seasonal variations, especially between winter and summer periods (Fig. 1). Significantly (Mann-Whitney test, $p < 0.001$), the summer period (considered the months of Apr. 2013; Jul. 2013, Aug. 2013, Sep. 2013 and Ap. 2014) presented more positive $\delta^{13}\text{C}$ -DIC signatures than the winter period (Oct. 2013, Dec. 2013, Jan. 2014 and Feb. 2014). Indeed, the average signatures of $\delta^{13}\text{C}$ -DIC for the entire bay in winter and summer were, respectively, $1.0\text{‰} \pm 1.4\text{‰}$ and $1.5\text{‰} \pm 1.7\text{‰}$. Moreover, the differences between surface and bottom waters for $\delta^{13}\text{C}$ -DIC during summer were of high statistical significance ($p < 0.001$; Wilcoxon test). DIC pool was significantly enriched in ^{13}C at the surface layer, as $\delta^{13}\text{C}$ -DIC averaged at $1.8\text{‰} \pm 0.6\text{‰}$ in surface waters and $1.2\text{‰} \pm 1.0\text{‰}$ in bottom waters (Table S1, supplementary file).

The Spearman correlation matrix was calculated for all the parameters considered in this study: $\delta^{13}\text{C}$ -DIC, salinity, temperature, Chl *a*, DIC, $p\text{CO}_2$, DO, photosynthetically active radiation (PAR), suspended particulate material (SPM), and particulate organic carbon (POC) (Table S2, supplementary file). The values were established with averages for each sampling campaign. Interestingly, $\delta^{13}\text{C}$ -DIC was significantly and positively correlated to temperature, Chl *a*, PAR, DO, SPM and POC concentrations, while negatively correlated to $p\text{CO}_2$ levels and DIC concentrations.

Fig. 2 showed the calculated diel photosynthetic fractionation factor (ϵ -DIC) plotted against the discrete values of $p\text{CO}_2$ and DIC concentrations. This approach was applied only at the diel scale, assuming that the phytoplankton blooms realized isotopic fractionation by incorporating preferentially the lighter stable carbon isotope. We compare the isotopic discrimination between the morning and the

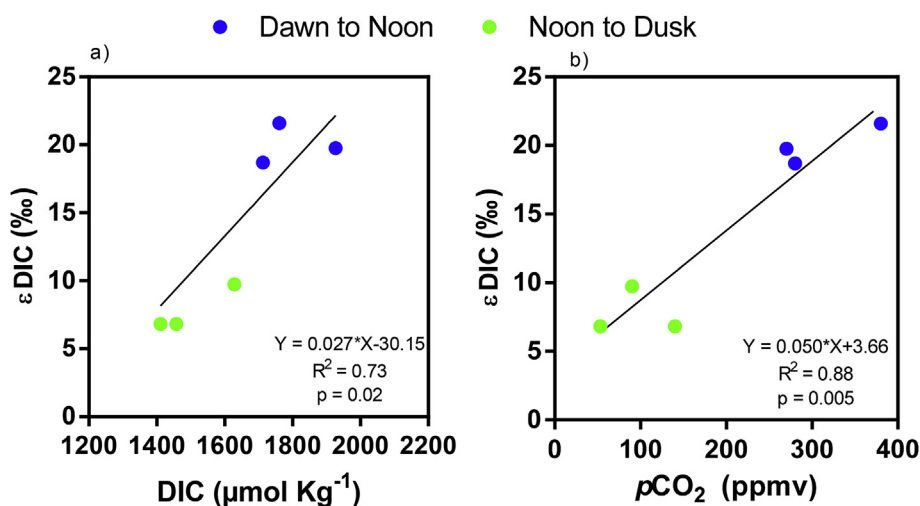


Fig. 2. Calculated apparent diel phytoplankton fractionation of $\delta^{13}\text{C}$ -DIC (ϵ -DIC) plotted against a) $p\text{CO}_2$ values and b) DIC concentrations. The blue circles represent the ϵ -DIC for the period from dawn to noon, and the green circles represent the ϵ -DIC for the period from noon to dusk. (For interpretation of the references to color in this figure legend, the reader is referred to the Web version of this article.)

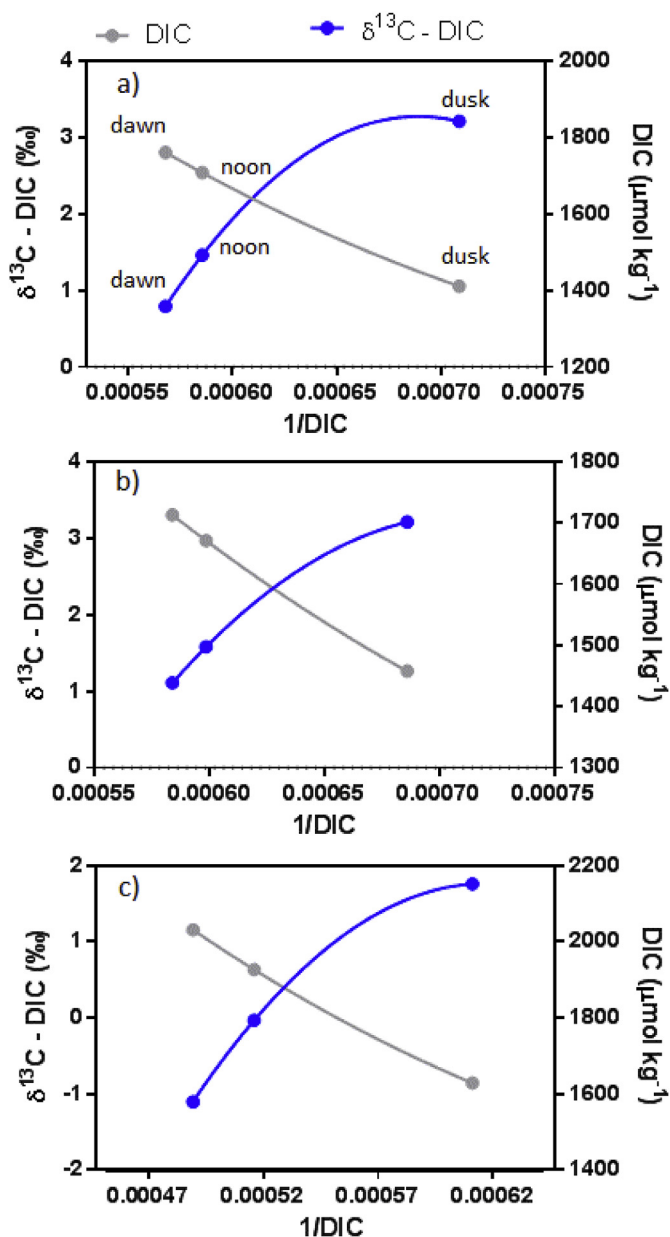


Fig. 3. Plots showing the diel variations of $\delta^{13}\text{C-DIC}$ and DIC (Rayleigh Distillation), where the increases of $\delta^{13}\text{C-DIC}$ values are equivalent to decreases in the DIC concentrations. Graphs a, b and c are represent the diel surveys (from dawn to dusk) in the months of Sep. 2013, Jan. 2014 and Apr. 2014, respectively.

afternoon. The isotopic fractionation was higher during the morning, ranging from 18.7‰ to 21.6‰ whereas lower fractionations occurred during the afternoon, and ranged between 6.8‰ and 11.1‰ (Fig. 2). The apparent photosynthetic fractionation factor was strongly and positively correlated to the concentrations of DIC ($R^2 = 0.73$, $p = 0.02$) and $p\text{CO}_2$ ($R^2 = 0.88$, $p < 0.005$) (Fig. 2). Fig. 3 showed the plots of Rayleigh distillation that aimed to better analyze the diel isotopic fractionation dynamic. The increase of $\delta^{13}\text{C-DIC}$ was related to a given change in the fraction of consumed DIC. The diel cycles of production and respiration caused $\delta^{13}\text{C-DIC}$ to vary between 2.1‰ and 2.8‰ (Fig. 3). The increase of $\delta^{13}\text{C-DIC}$ signatures along the day was proportional to the decrease of DIC concentrations (Fig. 3). The relationship between $\delta^{13}\text{C-DIC}$ and the Chl *a* concentrations was plotted using the sector-averaged values for each sampling survey (Fig. 4). This figure shows a positive relationship between the phytoplankton biomass and

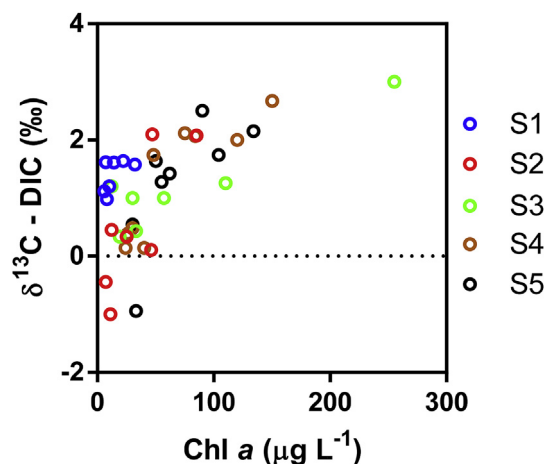


Fig. 4. Relationship between $\delta^{13}\text{C-DIC}$ signatures and Chl *a* concentrations. The graph present the averaged-sector values for each sampling campaign.

$\delta^{13}\text{C-DIC}$, especially at the most productive regions of Guanabara Bay (sectors 3, 4 and 5), where the extreme positive $\delta^{13}\text{C-DIC}$ signatures occurred in dense phytoplankton blooms with Chl *a* concentrations above $50 \mu\text{g L}^{-1}$ (Fig. 4).

The comparison of $\delta^{13}\text{C-DIC}$ signatures of Guanabara Bay with other ecosystems worldwide was provided in Fig. 5. Guanabara Bay showed an inverse tendency between $\delta^{13}\text{C-DIC}$ and $p\text{CO}_2$ values (Fig. 5a), where phytoplankton-dominated waters presented the highest $\delta^{13}\text{C-DIC}$ and the lowest $p\text{CO}_2$ values. The values of $p\text{CO}_2$ in Guanabara Bay were generally lower than the compiled data, whereas $\delta^{13}\text{C-DIC}$ signatures were much higher (Fig. 5a). This comparison of Guanabara Bay with other coastal and open ocean waters worldwide was also performed considering the salinity (Fig. 5b and c). These graphs showed a high scattering in the distributions of the $\delta^{13}\text{C-DIC}$ according to salinity. For a same salinity, the $\delta^{13}\text{C-DIC}$ may exhibit variation up to 20‰. The range of $\delta^{13}\text{C-DIC}$ was higher in low salinity regions and decreased progressively when freshwaters mixed with ocean waters. The salinity range between 20 and 30 presented the highest $\delta^{13}\text{C-DIC}$ enrichment in Guanabara Bay compared to the data from other estuaries and coasts, with a difference of about 3.20‰, on average (Fig. 5b). Compared to mangrove-dominated estuaries with salinities ranging from 15 to 20, Guanabara Bay showed a significant (Mann Whitney test, $p < 0.0001$) increase in $\delta^{13}\text{C-DIC}$ of 6.75‰ (Fig. 5b).

4. Discussion

4.1. Sewage inputs of depleted $\delta^{13}\text{C-DIC}$

As a coastal embayment dominated by saline waters, the inputs of freshwater to Guanabara Bay are very low compared to its water volume (Kjerfve et al., 1997). Taking account this hydrological characteristic, we calculated the sinks and sources of DIC and TA to the system for a special case, i.e., when the freshwater inputs are weak, following the procedures described by Jiang et al. (2008). Thus, it is possible to infer the gains and losses of DIC ($\Delta\text{DIC}_{\text{excess}}$) and TA ($\Delta\text{TA}_{\text{excess}}$) relative to the conservative mixing (see materials and methods for details). The maximum values of $\Delta\text{DIC}_{\text{excess}}$ and $\Delta\text{TA}_{\text{excess}}$ were coincident with the highest values of $p\text{CO}_2$ and no related to salinity (Fig. S2; supplementary file). Oversaturation of $p\text{CO}_2$ in the bay was restricted to sites close to the small river mouths and sewage channels (Cotovicz et al., 2015). These polluted sites present occasional occurrence of hypoxia and anoxia events, sustaining heterotrophic metabolism (Ribeiro and Kjerfve, 2002; Cotovicz et al., 2015). Anaerobic processes including ammonification, denitrification and sulphate reduction can contribute to the production of alkalinity (Abril and

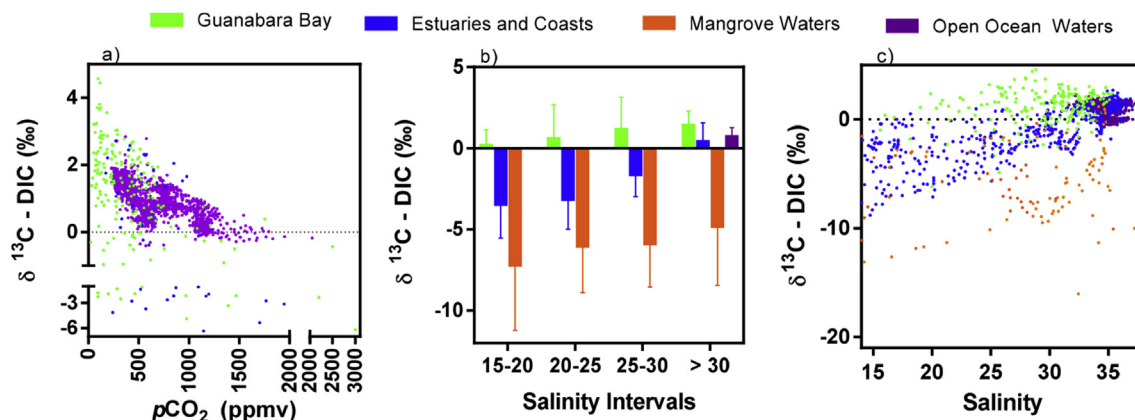


Fig. 5. Comparison of Guanabara Bay with other systems worldwide: a) relationship between $\delta^{13}\text{C-DIC}$ and $p\text{CO}_2$ values; b) distributions of $\delta^{13}\text{C-DIC}$ according to salinity intervals; c) distributions of $\delta^{13}\text{C-DIC}$ values against salinity. The references of the compiled data set are provided in the supplementary file.

Frankignoulle, 2001; Hu and Cai, 2011).

The spatial distributions of $\delta^{13}\text{C-DIC}$ along Guanabara Bay shows a higher ^{13}C depletion (down to -6.17‰) only closest to the locations that receive these direct inputs of DIC from effluent discharges (Fig. 1). Fig. 6 shows the plot of $\Delta\text{DIC}_{\text{excess}}/\text{DIC}_{\text{ocean}}$ against $\Delta\delta^{13}\text{C-DIC}$, and the slopes of this relationship can be used to infer the main biogeochemical processes affecting the distributions of DIC and $\delta^{13}\text{C-DIC}$ (see the figure caption for further explanations). The highest DIC additions occurred closest to Rio de Janeiro city at the northwestern region of Guanabara Bay (Sector 2). These samples from polluted sites fall within the III quadrant of the graph, indicating processes of organic carbon degradation (Samanta et al., 2015; Yang et al., 2018). For very high $p\text{CO}_2$ values, the data in quadrant III follows the theoretical slopes of wastewater contribution (slope = -0.012 ; vector D) and the degradation of organic carbon (slope = -0.020 ; vector C), and confirms the DIC inputs more depleted in ^{13}C . These polluted regions present the highest bacterial and virus contents (Fistarov et al., 2015), are sources of CO_2 and CH_4 (Cotovicz et al., 2015, 2016b), and show episodic evidence of corrosive waters with low saturation state of calcium carbonates (Cotovicz et al., 2018b). Similar results were found in the urbanized temperate Jiaozhou Bay-China (Yang et al., 2018), where the authors found an important input of depleted $\delta^{13}\text{C-DIC}$ in waters that receive direct discharge from wastewater plants.

The strong negative correlation ($R^2 = 0.8$; $p\text{-value} < 0.001$) between $\delta^{13}\text{C-DIC}$ and PO_4^{3-} in sector 2 reinforce the role of wastewaters as the main source of PO_4^{3-} and DIC depleted in ^{13}C in this region (Fig. S3; supplementary file). Studies have shown that, in general, the PO_4^{3-} -P was the dominant limiting nutrient in the bay, presenting sometimes an almost depletion and related to the strong phytoplankton uptake (Costa-Santos, 2015; Brandini et al., 2016). The calculated isotopic signature of the added DIC for the samples located in these polluted regions (excluding the data with $\text{Chl } a$ concentrations $> 50 \mu\text{g L}^{-1}$) gives a stable isotopic signature of sewage source of -12.2‰ (Fig. S2). This value is very consistent with that found in wastewater treatment plants in China (average of -12‰ ; Yang et al., 2018), and with values found in a domestic sewage emissary in another region of Rio de Janeiro city (-13‰ ; unpublished data). Taking into account this, we quantified the contribution of sewage discharges for the two most polluted regions (sectors 2 and 5; Fig. 1) by applying a simple two-source mixing model (Phillips and Gregg, 2001). We used the value of -12.2‰ as the $\delta^{13}\text{C-DIC}$ signature of sewage source, and the value of 1.5‰ as the $\delta^{13}\text{C-DIC}$ -signature source of marine source (considered the average $\delta^{13}\text{C-DIC}$ signature of sector 1). The model calculated a sewage contribution of about 10% in sector 2 and 5% in sector 5. The depleted $\delta^{13}\text{C-DIC}$ signature from polluted sources is lost very fast in the bay, confirming the sewage-derived DIC is rapidly degassed and/or assimilated by phytoplankton blooms, as we will discuss in the next

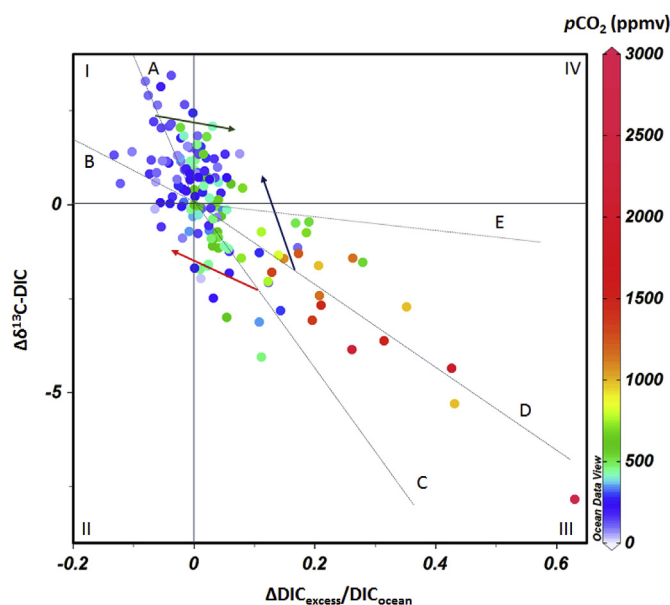


Fig. 6. Plot of $\Delta\delta^{13}\text{C-DIC}$ vs. $\Delta\text{DIC}_{\text{excess}}/\text{DIC}_{\text{ocean}}$ in the Guanabara Bay. The origin represents the conservative mixing with sample values equal to the ocean end-member value (see material and methods for further explanation). The four quadrants (I, II, III and IV) indicate additional processes that could influence the DIC and $\delta^{13}\text{C-DIC}$ distributions. The quadrant I represents the primary production/outgassing of CO_2 , when DIC concentrations increase and $\delta^{13}\text{C-DIC}$ values decrease. The quadrant II represents the calcite precipitation, when DIC concentrations and $\delta^{13}\text{C-DIC}$ values decrease. The quadrant III represents the degradation of organic carbon and inputs from wastewater, when DIC concentrations increase and $\delta^{13}\text{C-DIC}$ decrease. The quadrant IV represents the carbonate dissolution, when the DIC concentrations and the values of $\delta^{13}\text{C-DIC}$ increase. The vectors A, B, C, D and E represent the slopes of specific processes affecting the DIC and $\delta^{13}\text{C-DIC}$ distributions, that are, respectively, primary production (slope = -20.0‰), the outgassing of CO_2 (slope = -9.2‰), degradation of organic carbon (slope = -20.0‰), wastewater input of DIC (-12.2‰) and intrusion of atmospheric CO_2 (slope = -2.0‰). The red, blue and green arrows represent the direction in which the samples will follow if they are subject to more than one process. The red arrow represents the effect of organic matter degradation followed by outgassing of CO_2 , which is drawn parallel to vector B. The blue arrow represents the effect of degradation of organic carbon followed by biological production, which is drawn parallel to vector A. The green arrow represents the effect of primary production followed by intrusion of atmospheric CO_2 due to the air-water gradient, which is drawn parallel to vector E. (For interpretation of the references to color in this figure legend, the reader is referred to the Web version of this article.)

section of the manuscript. Important to point that the degassing is a process that turns the water more enriched in the heavier carbon isotope (^{13}C), since that during CO_2 emissions the lighter carbon (^{12}C) is preferentially emitted due to the kinetic isotope effect.

Another source of DIC depleted in ^{13}C to the water column in Guanabara Bay could be the mangrove forest located at the north-eastern region (Fig. 1); however, we could not find a clear contribution into the bay (except for one sample collected close to the region, during low tide, which presented a negative $\delta^{13}\text{C}$ -DIC signature of -2.5‰). This value is very far from that found in mangrove-dominated waters, for example, in a tidal creek in Gazi Bay (Kenya) where the $\delta^{13}\text{C}$ -DIC values were very depleted ($\sim -8\text{‰}$) even for salinities higher than 30 (Bouillon et al., 2007) (Fig. 5). This low influence of mangrove in Guanabara Bay occurs probably because of low tidal pumping related to the microtidal character of the bay (Cotovicz et al., 2018). In addition, the less ^{13}C -enriched sediments were restricted to the area very close to the mangrove forest (Carreira et al., 2002).

4.2. Influence of the phytoplankton fractionation on the $\delta^{13}\text{C}$ -DIC dynamics

Despite the influence of wastewater contribution closest to sites that receive direct sewage discharge, most of $\delta^{13}\text{C}$ -DIC values are positive, indicating an isotopic fractionation of DIC by marine phytoplankton by a preferential use of ^{12}C during photosynthesis (Fig. 6). Many data points follow the theoretical slope of primary production (represented by vector A) that decreases the ratio $\Delta\text{DIC}_{\text{excess}}/\text{DIC}_{\text{ocean}}$ and increases the $\Delta\delta^{13}\text{C}$ -DIC in the quadrant I (slope of -0.020). The high incidence of PAR, especially during summer, associate with high nutrient availability and formation of thermohaline stratification, increases the rates of primary production (Rebello et al., 1988), associated with development of massive phytoplankton blooms and strong CO_2 uptake (Cotovicz et al., 2015). This uptake of DIC removes preferentially the lighter ^{12}C , enriching the waters with the heavier stable carbon isotope (Mook, 2001). Successive algal blooms could consumes more of the DIC pool, and the residual DIC becomes progressively ^{13}C -enriched due to the isotopic fractionation (Finlay and Kendall, 2007). Guanabara Bay showed persistent phytoplankton blooms in all the sampling campaigns, which spread to the entire bay and cover larger areas during summer months (Cotovicz et al., 2015). Fig. 4 corroborates this result, with a positive tendency between the $\delta^{13}\text{C}$ -DIC and Chl *a* concentrations, suggesting that the seasonal variation of the $\delta^{13}\text{C}$ -DIC signature is related to changes in the extension of the phytoplankton dominance. This feature was also reported in the Perdido Estuary (Florida, USA) during periods of higher phytoplankton production (Coffin and Cifuentes, 1999), in the Scheldt Estuary (Netherlands and Belgium) when the $\delta^{13}\text{C}$ -DIC showed higher signatures during phytoplankton bloom periods (Hellings et al., 2001; Gillikin et al., 2006).

Fig. 6 presents some points located in the quadrant IV, which represents the carbonate dissolution. The process of carbonate dissolution consumes DIC of the water column, and adds $\delta^{13}\text{C}$ with an isotopic signature closest to that of marine carbonates (0‰), turning the waters enriched in ^{13}C relative to the conservative mixing (Alling et al., 2012). However, this process is unlikely to occur in the bay since that the values of $p\text{CO}_2$ in quadrant IV are low and the pH values are high (Cotovicz et al. 2018b). Actually, DIC and $\delta^{13}\text{C}$ -DIC can be subjected simultaneously to more than one process and not just by a specific one (Samanta et al., 2015). This means that if one sample was subject to degradation of organic carbon (represented by quadrant III) followed by primary production (represented by quadrant I), this sample could finally be located in quadrant IV (the deviation is represented by the blue arrow, which is drawn parallel to vector A). Similarly, if a sample was subject to the DIC uptake by primary production (vector A) and thereafter occurs an intrusion of atmospheric CO_2 due to the gradient at the air-water interface (CO_2 sink, vector E), this sample could also be deviated to the quadrant IV (green arrow). The red arrow is drawn parallel to vector B, representing the effect of organic carbon

degradation followed by outgassing of CO_2 . This is probably occurring in samples mainly from sector 2 that are located on quadrant IV that present high values of measured $p\text{CO}_2$, when the outgassing could be important due to important air-water gradient of CO_2 . Another example is the quadrant I, where exists two vectors (A and B), representing the slopes of biological production and outgassing, respectively. Both these processes lead to loss of DIC and increase of $\delta^{13}\text{C}$ -DIC. However, the process of outgassing in these samples are unlikely since that the values of $p\text{CO}_2$ in this quadrant are highly under-saturated.

The apparent phytoplankton isotopic fractionation (ϵ -DIC) was higher under conditions of high availability of dissolved CO_2 , with higher fractionation during the morning than the afternoon (Fig. 2). During morning, the values of $p\text{CO}_2$ were higher in Guanabara Bay as the results of the accumulated CO_2 respired during the nighttime (Cotovicz et al., 2015). This suggests that the discrimination against ^{13}C is higher when the availability of dissolved CO_2 is higher. Previous studies showed similar results, both in culture experiments (Fogel and Cifuentes, 1993), and *in situ* at a Chinese hypereutrophic lake (Van Dam et al., 2018). The $\delta^{13}\text{C}$ -DIC fractionation by phytoplankton in Guanabara Bay follows a Rayleigh distillation (Fig. 3), where the increasing removal of DIC fractions is accompanied by the isotopic fractionation of $\delta^{13}\text{C}$ -DIC, turning the water enriched in ^{13}C . The values of ϵ -DIC found during the morning period in Guanabara Bay were about 20‰ , a classical value for the marine phytoplankton (Fontugne and Duplessy, 1981; Fogel and Cifuentes, 1993; Mook, 2001). Under conditions of low $p\text{CO}_2$, the $\delta^{13}\text{C}$ -DIC fractionation decreases during the afternoon, reflecting the decline in carbon assimilation efficiency. This decrease of fractionation under CO_2 limitation was showed experimentally for marine diatoms (Burkhardt et al., 1999), and it is consistent with results found in a hypertrophic Chinese lake under conditions of CO_2 sub saturation (Van Dam et al., 2018). In addition, under low availability of dissolved CO_2 , the phytoplankton can consumes bicarbonate (HCO_3^-) (Burns and Beardall, 1987), and this could contribute to decrease the isotopic fractionation factor since that the isotope ratio of HCO_3^- is about 8‰ more positive than that of dissolved CO_2 (Fogel and Cifuentes, 1993). Previous studies suggested an active uptake of HCO_3^- in Guanabara Bay due to the enrichment of the $\delta^{13}\text{C}$ -POC pool ($\delta^{13}\text{C}$ -POC reaching -15.1‰ ; Kalas et al., 2009; Martins et al., 2016). Cyanobacteria blooms, which have already been documented in Guanabara Bay, can use bicarbonate under low $p\text{CO}_2$ availability (Miller et al. 1990).

4.3. Comparison with other ecosystems worldwide

The plot of $\delta^{13}\text{C}$ -DIC versus $p\text{CO}_2$ (Fig. 5a) shows that the blooms-dominated waters present strong $p\text{CO}_2$ under-saturation and are as well enriched in ^{13}C , that is intrinsically related to the extreme levels of primary production. Guanabara Bay presented values of $\delta^{13}\text{C}$ -DIC high above than those of the compiled data in estuaries and coasts, revealing the advanced process of eutrophication in the bay. The compiled data in estuaries presented a high scattering compared to the open ocean waters, especially for values of $\delta^{13}\text{C}$ -DIC lower than 0‰ (Fig. 5c). This reflects a combination of processes such as respiration of terrestrial organic carbon from multiple sources with different $\delta^{13}\text{C}$ signatures, weathering and the contribution of carbonate rocks in the watershed, primary production, gas exchange and water mixing along the land-ocean aquatic continuum (Mook, 2001). The matrix correlation (Table S2) shows that higher values of $\delta^{13}\text{C}$ -DIC are related to high levels of DO, POC, SPM, and Chl *a*, and low concentrations of DIC. Recent findings in Guanabara Bay showed that the DOC and POC fractions present a large phytoplankton dominance, surpassing the contribution of terrestrial sources (Cotovicz et al. 2018a). Compared to other estuaries, Guanabara Bay presented the highest enrichment of ^{13}C -DIC in the salinity range between 20 and 30 (Fig. 5b). In Guanabara Bay, this salinity interval is present in confined stratified waters of the sectors 3, 4 and 5, which are net autotrophic and phytoplankton-dominated

(Rebello et al. 1988; Cotovicz et al., 2015, 2018a). This behavior is in contrast with most of other estuarine studies, which are mostly located in temperate regions and river-dominated ecosystems, where the effects of respiration, either in the water column or in sediments, are often much more pronounced than photosynthesis (Mook, 2001; Bouillon et al., 2003). The relative enrichment of ^{13}C -DIC is also important for salinities > 30 , suggesting that Guanabara Bay can export ^{13}C -DIC enriched waters to the coastal ocean. There is a marked depletion of $\delta^{13}\text{C}$ -DIC in estuaries dominated by mangroves. The net inputs of ^{13}C -depleted DIC in mangroves are attributed to the predominance of respiration in tidal creeks, as this process adds DIC to the water with a signature similar to that of the organic matter being respired (C3 plants with signature ranging between -24% and -30%) (Bouillon et al., 2003; Bouillon et al. 2011; Miyajima et al., 2009).

In open ocean waters, the compiled data of $\delta^{13}\text{C}$ -DIC showed a range between -1.13% and 2.31% , averaging at $0.70\% \pm 0.57\%$ (Fig. 5). This range of $\delta^{13}\text{C}$ -DIC is in accordance with previous studies in seawaters with a limited influence from land carbon sources (-2.0% and 2.0% ; Mook and Tan, 1991). However, the average of 0.71% is slightly lower than previous averages reported in literature (Kroopnick, 1985; Mook, 2001). According to Mook (2001), the $\delta^{13}\text{C}$ -DIC in seawater varies between $+0.0\%$ and $+2.5\%$, with the majority of data between 1.0% and 2.0% . According to Kroopnick (1985), the $\delta^{13}\text{C}$ -DIC of surface oceanic waters are generally around 2.0% . Differences in the averages and ranges of these studies can be attributed to the specific conditions during sampling collection, since that consider regions with distinct biological, air-sea exchange processes and different *in situ* temperatures, which could alter the $\delta^{13}\text{C}$ -DIC signature. In addition, $\delta^{13}\text{C}$ -DIC could substantially differ considering the differences between surface and bottom waters. $\delta^{13}\text{C}$ -DIC can present vertical stratification attributed to the oxidation of the organic material produced at the surface waters (majority from phytoplanktonic origin) as it falls through the water column and remineralizes at depth, with addition of isotopically light respiratory CO_2 to the DIC pool below the pycnocline (Kroopnick, 1985; Koné et al., 2009; Eide et al., 2017). Lower $\delta^{13}\text{C}$ -DIC values in bottom waters were reported in several estuarine, coastal and open ocean waters (Chou et al., 2007; Burt et al., 2016; Humphreys et al., 2016; Filipsson et al., 2017). Guanabara Bay also present a significant vertical $\delta^{13}\text{C}$ -DIC stratification during summer, with higher values at surface waters, reflecting the enrichment by phytoplankton blooms, and the depletion in bottom waters due to the predominance of respiration of organic matter (Table S1).

5. Conclusion

Our results showed a strong control of $\delta^{13}\text{C}$ -DIC dynamics by biological processes in the highly polluted and eutrophic Guanabara Bay. Indeed, the extreme high Chl *a* concentrations concomitant with heavier $\delta^{13}\text{C}$ -DIC signatures and low $p\text{CO}_2$ values indicate a strong carbon isotopic fractionation by primary production, especially at mid-inner shallow regions of the bay. The isotopic fractionation induced by primary production is accentuated during summer conditions when the vertical thermohaline stratification, the nutrients availability and the photosynthetically active radiation were at their highest. Our calculated apparent phytoplankton fractionation based on diel variations of $\delta^{13}\text{C}$ -DIC signatures and DIC concentrations showed higher ^{13}C discrimination from morning to noon period, decreasing during afternoon, following a Rayleigh distillation process. Overall, the *in situ* $\delta^{13}\text{C}$ -DIC concentrations were well above than the values expected in equilibrium with atmospheric CO_2 concentrations. The lower/negative $\delta^{13}\text{C}$ -DIC signatures were restricted to the regions under direct influence of domestic effluent discharges, where high inputs of organic matter stimulate the microbial respiration that adds depleted $\delta^{13}\text{C}$ -DIC into the waters. The process of air-water exchange seems also to exert influence on the isotope signatures; however, in a lower magnitude compared to the biological activities. Compared to the compiled data from several

estuaries and open ocean waters worldwide, Guanabara Bay showed a marked enrichment of ^{13}C , increasing $\delta^{13}\text{C}$ -DIC signatures. The highest signature of $\delta^{13}\text{C}$ -DIC in Guanabara Bay reached 4.57% , and to the best of our knowledge, this is the highest value reported in coastal and open waters worldwide. These results indicate that the eutrophication process can deeply modify the isotopic signature of the dissolved inorganic carbon pool in coastal waters dominated by large algal blooms.

Acknowledgments

This study was supported by the No Frontier Sciences Program of the Brazilian National Council of Research and Development (CNPq-PVE No 401.726/2012-6), by the Carlos Chagas Foundation for Research Support of the State of Rio de Janeiro (FAPERJ; proc. no. E-26202.785/2016), and by the Coordination for the Improvement of Higher Education Personnel (CAPES). Luiz C. Cotovicz Jr. is a post-doctoral researcher of FAPERJ (FAPERJ; proc. no. E-26202.785/2016); B. A. Knoppers is a senior scientist of CNPq (proc. no. 301572/2010-0). We are grateful to Nilva Brandini and Suzan J. Costa Santos (Federal Fluminense University) for their support during field sampling, and to Karine Charlier (Bordeaux University) for her support with IRMS analytical procedures. The symbols used in the graphical abstract are a courtesy of the Integration and Application Network, University of Maryland Center for Environmental Science (ian.umces.edu/symbols/).

Appendix A. Supplementary data

Supplementary data to this article can be found online at <https://doi.org/10.1016/j.ecss.2019.02.048>.

References

- Abril, G., Frankignoulle, M., 2001. Nitrogen – alkalinity interactions in the highly polluted Scheldt Basin (Belgium). *Water Res.* 35, 844–850.
- Alling, V., Porcelli, D., Mörth, C.M., Anderson, L.G., Sanchez-Garcia, L., Gustafsson, Ö., Andersson, P.S., Humborg, C., 2012. Degradation of terrestrial organic carbon, primary production and out-gassing of CO_2 in the Laptev and East Siberian Seas as inferred from $\delta^{13}\text{C}$ values of DIC. *Geochem. Cosmochim. Acta* 95, 143–159. <https://doi.org/10.1016/j.gca.2012.07.028>.
- Bauer, J.E., Cai, W.-J., Raymond, P., Bianchi, T.S., Hopkinson, C.S., Regnier, P., 2013. The changing carbon cycle of the coastal ocean. *Nature* 504 (7478), 61–70. <https://doi.org/10.1038/nature12857>.
- Bhavaya, P.S., Kumar, S., Gupta, G.V.M., Sudharma, K.V., Sudheesh, V., 2018. Spatio-temporal variation in $\delta^{13}\text{C}$ -DIC of a tropical eutrophic estuary (Cochin estuary, India) and adjacent Arabian Sea. *Cont. Shelf Res.* 153, 75–85. <https://doi.org/10.1016/j.csr.2017.12.006>.
- Bidone, E.D., Lacerda, L.D., 2004. The use of DPSIR framework to evaluate sustainability in coastal areas, case study: Guanabara Bay Basin, Rio de Janeiro, Brazil. *Reg. Environ. Change* 4, 5–16. <https://doi.org/10.1007/s10113-003-0059-2>.
- Borges, A.V., 2005. Do we have enough pieces of the jigsaw to integrate CO_2 fluxes in the coastal ocean? *Estuaries* 28, 3–27. <https://doi.org/10.1007/BF02732750>.
- Borges, A.V., Abril, G., 2011. Carbon dioxide and methane dynamics in estuaries. In: Wolanski, E., McLusky, D. (Eds.), *Treatise on Estuarine and Coastal Science*. Academic Press, Amsterdam, pp. 119–161.
- Bouillon, S., Frankignoulle, M., Dehairs, F., Velimirov, B., Eiler, A., Abril, G., Etcheber, H., Borges, A.V., 2003. Inorganic and organic carbon biogeochemistry in the Gautami Godavari estuary (Andhra Pradesh, India) during pre-monsoon: the local impact of extensive mangrove forests. *Glob. Biogeochem. Cycles* 17. <https://doi.org/10.1029/2002GB002026>.
- Bouillon, S., Dehairs, F., Schiettecatte, L.-S., Borges, A.V., 2007. Biogeochemistry of the Tana estuary and delta (northern Kenya). *Limnol. Oceanogr.* 52 (1), 46–59. <https://doi.org/10.4319/lo.2007.52.1.0046>.
- Bouillon, S., Connolly, R.M., Gillikin, D.P., 2011. Use of stable isotopes to understand food webs and ecosystem functioning in estuaries. In: Wolanski, E., McLusky, D. (Eds.), *Treatise on Estuarine and Coastal Science*. Academic Press, Amsterdam, pp. 143–173.
- Brandini, N., Rodrigues, A.P.C., Abreu, I.M., Cotovicz Jr., L.C., Knoppers, B.A., Machado, W.V., 2016. Nutrient behavior in a highly-eutrophicated tropical estuarine system. *Acta Limnol. Bras.* 28 e-21. <https://doi.org/10.1590/S2179-975X3416>.
- Burkhardt, S., Riebesell, U., Zondervan, L., 1999. Effects of growth rate, CO_2 concentration, and cell size on the stable carbon isotope fractionation in marine phytoplankton. *Geochem. Cosmochim. Acta* 63 (22), 3729–3741. [https://doi.org/10.1016/S0016-7037\(99\)00217-3](https://doi.org/10.1016/S0016-7037(99)00217-3).
- Burns, B.D., Beardall, J., 1987. Utilization of inorganic carbon acquisition by marine microalgae. *J. Exp. Mar. Biol. Ecol.* 107, 75–86.
- Burt, W.J., Thomas, H., Hagens, M., Pätzsch, J., Clargo, N.M., Salt, L.A., Winde, V.,

- Böttcher, M.E., 2016. Carbon sources in the North Sea evaluated by means of radium and stable carbon isotope tracers. *Limnol. Oceanogr.* 61, 666–683. <https://doi.org/10.1002/lno.10243>.
- Cai, W.-J., Wang, Y., 1998. The chemistry, fluxes, and sources of carbon dioxide in the estuarine waters of the Satilla and Altamaha Rivers, Georgia. *Limnol. Oceanogr.* 43 (4), 657–668.
- Campeau, A., Wallin, M.B., Giesler, R., Löfgren, S., Mörth, C.M., Schiff, S., Venkateswaran, J.J., Bishop, K., 2017. Multiple sources and sinks of dissolved inorganic carbon across Swedish streams, refocusing the lens of stable C isotopes. *Sci. Rep.* 7, 1–14. <https://doi.org/10.1038/s41598-017-09049-9>.
- Carreira, R.S., Wagener, A.L.R., Readman, J.W., Fileman, T.W., Macko, S.A., Veiga, A., 2002. Changes in the sedimentary organic carbon pool of a fertilized tropical estuary, Guanabara Bay, Brazil: an elemental, isotopic and molecular marker approach. *Mar. Chem.* 79, 207–227. [https://doi.org/10.1016/S0304-4203\(02\)00065-8](https://doi.org/10.1016/S0304-4203(02)00065-8).
- Chanton, J.P., Lewis, F.G., 1999. Plankton and dissolved inorganic carbon isotopic composition in a river-dominated estuary: apalachicola bay, Florida. *Estuaries* 22 (3), 575. <https://doi.org/10.2307/1353045>.
- Chen, C.-T.A., Huang, T.-H., Chen, Y.-C., Bai, Y., He, X., Kang, Y., 2013. Air–sea exchanges of CO₂ in the world's coastal seas. *Biogeosciences* 10, 6509–6544. <https://doi.org/10.5194/bg-10-6509-2013>.
- Chou, W.C., Sheu, D.D., Lee, B.S., Tseng, C.M., Chen, C.T.A., Wang, S.L., Wong, G.T.F., 2007. Depth distributions of alkalinity, TCO₂ and $\delta^{13}\text{C}_{\text{TCO}_2}$ at SEATS time-series site in the northern South China Sea. *Deep. Res. Part II Top. Stud. Oceanogr.* 54, 1469–1485. <https://doi.org/10.1016/j.dsr.2.2007.05.002>.
- Coffin, R.B., Cifuentes, L.A., 1999. Stable isotope analysis of carbon cycling in the Perdido estuary, Florida. *Estuaries* 22 (4), 917–926.
- Costa-Santos, S.J., 2015. Determinação do estado trófico a partir da aplicação dos índices O'Boyle e TRIX nos compartimentos da Baía de Guanabara, RJ. Master Dissertation. Federal Fluminense University, Brazil WWW Page. https://app.uff.br/riuff/bitstream/1/1642/1/Dissertacao_Suzan%20Versao_10.1_VersaoFINAL.pdf.
- Cotoviz Jr., L.C., Knoppers, B.A., Brandini, N., Costa Santos, S.J., Abril, G., 2015. A strong CO₂ sink enhanced by eutrophication in a tropical coastal embayment (Guanabara Bay, Rio de Janeiro, Brazil). *Biogeosciences* 12 (20), 6125–6146. <https://doi.org/10.5194/bg-12-6125-2015>.
- Cotoviz Jr., L.C., Libardoni, B., Brandini, N., Knoppers, B., Abril, G., 2016a. Comparações entre medições em tempo real da pCO₂ aquática com estimativas indiretas em dois estuários tropicais contrastantes: o estuário eutrofizado da Baía de Guanabara (RJ) e o estuário oligotrófico do Rio São Francisco (AL). *Quím. Nova* 39, 1206–1214. <https://doi.org/10.21577/0100-4042.20160145.22>.
- Cotoviz Jr., L.C., Knoppers, B.A., Brandini, N., Poirier, D., Costa Santos, S.J., Abril, G., 2016b. Spatio-temporal variability of methane (CH₄) concentrations and diffusive fluxes from a tropical coastal embayment surrounded by a large urban area (Guanabara Bay, Rio de Janeiro, Brazil). *Limnol. Oceanogr.* 61, S238–S252. <https://doi.org/10.1002/lno.10298>.
- Cotoviz Jr., L.C., Knoppers, B.A., Brandini, N., Poirier, D., Costa Santos, S.J., Cordeiro, R.C., Abril, G., 2018a. Predominance of phytoplankton-derived dissolved and particulate organic carbon in a highly eutrophic tropical coastal embayment (Guanabara Bay, Rio de Janeiro, Brazil). *Biogeochemistry* 137, 1–14. <https://doi.org/10.1007/s10533-017-0405-y>.
- Cotoviz Jr., L.C., Knoppers, B.A., Brandini, N., Poirier, D., Costa Santos, S.J., Abril, G., 2018b. Aragonite saturation state in a tropical coastal embayment dominated by phytoplankton blooms (Guanabara Bay - Brazil). *Mar. Pollut. Bull.* 129 (2), 729–739. <https://doi.org/10.1016/j.marpolbul.2017.10.064>.
- Deirmendjian, L., Abril, G., 2018. Carbon dioxide degassing at the groundwater-stream-atmosphere interface: isotopic equilibration and hydrological mass balance in a sandy watershed. *J. Hydrol.* 558, 129–143. <https://doi.org/10.1016/j.jhydrol.2018.01.003>.
- Dickson, A.G., Millero, F.J., 1987. A comparison of the equilibrium constants for the dissociation of carbonic acid in seawater media. *Deep-Sea Res.* 34, 1733–1743.
- Eide, M., Olsen, A., Ninnemann, U., Johannessen, T., 2017. A global ocean climatology of preindustrial and modern ocean $\delta^{13}\text{C}$. *Glob. Biogeochem. Cycles* 31 (3), 515–534. <https://doi.org/10.1002/2016GB005473>.
- Filipsson, H.L., McCorkle, D.C., Mackensen, A., Bernhard, J.M., Andersson, L.S., Naustvoll, L.-J., Caballero-Alfonso, A.M., Nordberg, K., Danielssen, D.S., 2017. Seasonal variability of stable carbon isotopes ($\delta^{13}\text{C}_{\text{DIC}}$) in the Skagerrak and the Baltic Sea: distinguishing between mixing and biological productivity. *Palaeogeogr. Palaeoclimatol. Palaeoecol.* 483, 15–30. <https://doi.org/10.1016/j.palaeo.2016.11.031>.
- Finlay, J.C., Kendall, C., 2007. Stable isotope tracing of temporal and spatial variability in organic matter sources to freshwater ecosystems. In: Michener, R., Lajtha, K. (Eds.), *Stable Isotopes in Ecology and Environmental Science*. Blackwell Publishing, Hong Kong, pp. 594.
- Fistarol, G.O., Coutinho, F.H., Moreira, A.P.B., Venas, T., Cánovas, A., de Paula, S.E.M., Coutinho, R., de Moura, R.L., Valentin, J.L., Tenenbaum, D.R., Paranhos, R., do Valle, R.D., Vicente, A.C.P., Amado Filho, G.M., Pereira, R.C., Kruger, R., Rezende, C.E., Thompson, C.C., Salomon, P.S., Thompson, F.L., 2015. Environmental and sanitary conditions of Guanabara Bay, Rio de Janeiro. *Front. Microbiol.* 6, 1232. <https://doi.org/10.3389/fmicb.2015.011232>.
- Fogel, M.L., Cifuentes, L.A., 1993. Isotope fractionation during primary production. In: Engel, M.H., Macko, S.A. (Eds.), *Organic Geochemistry*. Plenum Press, New York, pp. 73–98.
- Fontugne, M.R., Duplessy, J.-C., 1981. Organic carbon isotopic fractionation by marine plankton in the temperature range -1 to 31°C. *Oecologia Acta* 4 (1), 85–90.
- Frankignoulle, M., Borges, A., Biondo, R., 2001. A new design of equilibrator to monitor carbon dioxide in highly dynamic and turbid environments. *Water Res.* 35, 1344–1347.
- Fry, B., 2002. Conservative mixing of stable isotopes across estuarine salinity gradients: a conceptual framework for monitoring watershed influences on downstream fisheries production. *Estuaries* 25 (2), 264–271. <https://doi.org/10.1007/BF02691313>.
- Gattuso, J.P., Frankignoulle, M., Wollast, R., 1998. Carbon and carbonate metabolism in coastal aquatic ecosystems. *Annu. Rev. Ecol. Systemat.* 29, 405–434. <https://doi.org/10.1146/annurev.ecolsys.29.1.405>.
- Gazeau, F., Smith, S.V., Gentili, B., Frankignoulle, M., Gattuso, J.-P., 2004. The European coastal zone: characterization and first assessment of ecosystem metabolism. *Estuar. Coast Shelf Sci.* 60 (4), 673–694. <https://doi.org/10.1016/j.ecss.2004.03.007>.
- Gillikin, D.P., Lorrain, A., Bouillon, S., Willenz, P., Dehairs, F., 2006. Stable carbon isotopic composition of *Mytilus edulis* shells: relation to metabolism, salinity, $\delta^{13}\text{C}_{\text{DIC}}$ and phytoplankton. *Org. Geochem.* 37 (10), 1371–1382. <https://doi.org/10.1016/j.orggeochem.2006.03.008>.
- Gran, G., 1952. Determination of the equivalence point in potentiometric titrations. *Part II. Analyst* 77 (920), 661–671.
- Grasshoff, K., Ehrhardt, M., Kremling, K., 1999. *Methods of Seawater Analysis*. Wiley-VCH.
- Gruber, N., Keeling, C.D., Bacastow, R.B., Guenther, P.R., Lueter, T.J., Wahlen, M., Meijer, H.A.J., Mook, W.G., Stocker, T.F., 1999. Spatiotemporal patterns of carbon-13 in the global surface oceans and the oceanic Suess Effect. *Glob. Biogeochem. Cycles* 13 (2), 307–335.
- Hellings, L., Dehairs, F., Van Damme, S., Baeyens, W., 2001. Dissolved inorganic carbon in a highly polluted estuary (the Scheldt). *Limnol. Oceanogr.* 46 (6), 1406–1414. <https://doi.org/10.4319/lo.2001.46.6.1406>.
- Hu, X., Cai, W.-J., 2011. An assessment of ocean margin anaerobic processes on oceanic alkalinity budget. *Glob. Biogeochem. Cycles* 25 n/a. <https://doi.org/10.1029/2010GB003859>.
- Humphreys, M., Greatrix, F., Tynan, E., Achterberg, E., Griffiths, A., Fry, C., Garley, R., McDonald, A., Boyce, A., 2016. Stable carbon isotopes of dissolved inorganic carbon for a zonal transect across the subpolar North Atlantic Ocean in summer 2014. *Earth Syst. Sci. Data* 8, 221–233. <https://doi.org/10.5194/essd-8-221-2016>.
- Hunt, C., Salisbury, J., Vandemark, D., McGillis, W., 2010. Contrasting Carbon Dioxide Inputs and Exchange in Three Adjacent New England Estuaries. *Estuaries and Coasts* 34, 68–77. <https://doi.org/10.1007/s12237-010-9299-9>.
- Inoue, H., Sugimura, Y., 1985. Carbon isotopic fractionation during the CO₂ exchange process between air and sea water under equilibrium and kinetic conditions. *Geochem. Cosmochim. Acta* 49, 2453–2460.
- Jiang, L.Q., Cai, W.-J., Wang, Y.C., 2008. A comparative study of carbon dioxide degassing in river- and marine-dominated estuaries. *Limnol. Oceanogr.* 53, 2603–2615. <https://doi.org/10.4319/lo.2008.53.6.2603>.
- Joeseof, A., Kirchman, D.L., Sommerfeld, C.K., Cai, W.-J., 2017. Seasonal variability of the inorganic carbon system in a large coastal plain estuary. *Biogeosciences* 14, 4949–4963. <https://doi.org/10.5194/bg-14-4949-2017>.
- Kalas, F.A., Carreira, R.S., Macko, S.A., Wagener, A.L.R., 2009. Molecular and isotopic characterization of the particulate organic matter from an eutrophic coastal bay in SE Brazil. *Cont. Shelf Res.* 29, 2293–2302. <https://doi.org/10.1016/j.csr.2009.09.007>.
- Kendall, C., Doctor, D.H., 2004. Stable isotope applications in hydrologic studies. In: Drever, J.I. (Ed.), *Surface and Ground Water, Weathering, and Soils: Treatise on Geochemistry*. vol. 5, pp. 319–364.
- Kjerfve, B., Ribeiro, C.A., Dias, G.T.M., Filippo, A., Quaresma, V.S., 1997. Oceanographic characteristics of an impacted coastal bay: baía de Guanabara, Rio de Janeiro, Brazil. *Cont. Shelf Res.* 17, 1609–1643.
- Koné, Y.J.M., Abril, G., Kouadio, K.N., Delille, B., Borges, A.V., 2009. Seasonal variability of carbon dioxide in the rivers and lagoons of Ivory Coast (West Africa). *Estuar. Coasts* 32, 246–260. <https://doi.org/10.1007/s12237-008-9121-0>.
- Kroopnick, P.M., 1985. The distribution of ^{13}C of ΣCO_2 in the world oceans. *Deep Sea Res. Part A, Oceanogr. Res. Pap.* 32 (1), 57–84. [https://doi.org/10.1016/0198-0149\(85\)90017-2](https://doi.org/10.1016/0198-0149(85)90017-2).
- Martins, J., Silva, T., Fernandes, A., Massone, C., Carreira, R., 2016. Characterization of particulate organic matter in a Guanabara Bay- coastal ocean transect using elemental, isotopic and molecular markers. *PANAMJAS* 11, 276–291.
- Mehrbach, C., Cuberson, C.H., Hawley, J.E., Pytkowicz, R.M., 1973. Measurements of the apparent dissociation constants of carbonic acid in seawater at atmospheric pressure. *Limnol. Oceanogr.* 18, 897–907 1973.
- Miller, J.D., Espie, G.S., Canvin, D.T., 1990. Physiological aspects of CO₂ and HCO₃ transport by cyanobacteria: a review. *Can. J. Bot.* 68, 1291–1302. <https://doi.org/10.1139/b90-165>.
- Miyajima, T., Miyajima, Y., Hanba, Y.T., Yoshii, K., Koitabashi, T., Wada, E., 1995. Determining the stable isotope ratio of total dissolved inorganic carbon in lake water by GC/C/IRMS. *Limnol. Oceanogr.* 40, 994–1000. <https://doi.org/10.4319/lo.1995.40.5.0994>.
- Miyajima, T., Tsuboi, Y., Tanaka, Y., Koike, I., 2009. Export of inorganic carbon from two Southeast Asian mangrove forests to adjacent estuaries as estimated by the stable isotope composition of dissolved inorganic carbon. *J. Geophys. Res. Biogeosciences* 114 (1), 1–12. <https://doi.org/10.1029/2008JG000861>.
- Mook, W.G., 2001. *Environmental Isotopes in the Hydrological Cycle. Principles and Applications*. UNESCO/IAEA Series, Paris.
- Mook, W.G., Tan, F.C., 1991. Stable carbon isotopes in rivers and estuaries. In: Degens, E.T., Kempe, S., Richey, J.E. (Eds.), *Biogeochemistry of Major World Rivers*. John Wiley and Sons, Chichester, UK, pp. 245–264.
- Phillips, D.L., Gregg, J.W., 2001. Uncertainty in source partitioning using stable isotopes. *Oecologia* 127, 171–179. <https://doi.org/10.1007/s004420000578>.
- Rau, G.H., Riebesell, U., Wolf-Gladrow, D., 1996. A model of photosynthetic C-13 fractionation by marine phytoplankton based on diffusive molecular CO₂ uptake. *Mar. Ecol. Prog. Ser.* 133, 275–285.
- Rebello, A.L., Ponciano, C.R., Melges, L.H., 1988. Avaliação da produtividade primária e da disponibilidade de nutrientes na Baía de Guanabara. *An. Acad. Bras. Cienc.* 60,

- 419–430.
- Ribeiro, C., Kjerfve, B., 2002. Anthropogenic influence on the water quality in Guanabara bay, Rio de Janeiro, Brazil. *Reg. Environ. Change* 3, 13–19. <https://doi.org/10.1007/s10113-001-0037-5>.
- Robbins, L.L., Hansen, M.E., Kleypas, J.A., Meylan, S.C., 2010. CO2 Calc: a user-friendly seawater carbon calculator for Windows, Mac OS X, and iOS (iPhone). U.S. Geological Survey Open-File Report, 2010–1280 1–17. available at: <http://pubs.usgs.gov/of/2010/1280/>.
- Samanta, S., Dalai, T.K., Pattanaik, J.K., Rai, S.K., Mazumdar, A., 2015. Dissolved inorganic carbon (DIC) and its $\delta^{13}\text{C}$ in the Ganga (Hooghly) River estuary, India: evidence of DIC generation via organic carbon degradation and carbonate dissolution. *Geochem. Cosmochim. Acta* 165, 226–248. <https://doi.org/10.1016/j.gca.2015.05.040>.
- Siegenthaler, U., Münnich, K.O., 1981. $^{13}\text{C}/^{12}\text{C}$ fractionation during CO_2 transfer from air to sea. In: Bolin, B. (Ed.), *SCOPE 16 - The Global Carbon Cycle*. Wiley & Sons, New York, pp. 249–257.
- Strickland, J.D.H., Parsons, T.R., 1972. *A Practical Handbook of Seawater Analysis*, second ed. Fisheries Research Board of Canada Bulletin.
- Van Dam, B.R., Tobias, C., Holbach, A., Paerl, H.W., Zhu, G., 2018. CO_2 limited conditions favor cyanobacteria in a hypereutrophic lake: an empirical and theoretical stable isotope study. *Limnol. Oceanogr.* 63, 1643–1659. <https://doi.org/10.1002/lno.10798>.
- Wang, X., Luo, C., Ge, T., Xu, C., Xue, Y., 2016. Controls on the sources and cycling of dissolved inorganic carbon in the Changjiang and Huanghe River estuaries, China: ^{14}C and ^{13}C studies. *Limnol. Oceanogr.* 61 (4), 1358–1374. <https://doi.org/10.1002/lno.10301>.
- Yang, X., Xue, L., Li, Y., Han, P., Liu, X., Zhang, L., Cai, W.-J., 2018. Treated wastewater changes the export of dissolved inorganic carbon and its isotopic composition and leads to acidification in coastal oceans. *Environ. Sci. Technol.* 52, 5590–5599. <https://doi.org/10.1021/acs.est.8b00273>.
- Zeebe, R.E., Wolf-Gladrow, D., 2001. *CO_2 in Seawater: Equilibrium, Kinetics, Isotopes*. Elsevier Oceanography Series, 65 Amsterdam.
- Zhang, J., Quay, P.D., Wilbur, D.O., 1995. Carbon isotope fractionation during gas-water exchange and dissolution of CO_2 . *Geochem. Cosmochim. Acta* 59 (1), 107–114. [https://doi.org/10.1016/0016-7037\(95\)91550-D](https://doi.org/10.1016/0016-7037(95)91550-D).